

Supporting Information

Direct electrocatalytic N-H aziridination of aromatic alkenes using ammonia

*Jef R. Vanhoof, Pieter J. De Smedt, Besir Krasniqi, Rob Ameloot, Dimitrios Sakellariou, Dirk E. De Vos**

*Centre For Membrane Separations, Adsorption, Catalysis and Spectroscopy for Sustainable Solutions (cMACS), KU Leuven, Celestijnenlaan 200F p.o. box 2454, 3001 Leuven (Belgium). E-mail: dirk.devos@kuleuven.be

Total number of pages: **32**

Total number of Figures: **17**

Total number of Tables: **5**

Total number of Equations: **1**

Table of Contents

1) General information	3
2) General procedure for the electrocatalytic aziridination	4
3) Optimization of the reaction conditions for styrene	8
4) Calculating the Faradaic efficiency; experiments in a divided cell	11
5) Spectrophotometry.....	14
6) Cyclic Voltammetry experiments.....	15
7) Spectroscopic data	18
8) References	31

1) General information

All reactions were carried out with commercially available chemicals and materials, unless otherwise noted. Chemicals were used without any further purification. ^1H -NMR analyses of the reaction mixtures were conducted with a Bruker Avance 300 spectrometer using a zg30 pulse program (1D ^1H experiment using 30 degree flip angle). 1D ^{15}N - $\{^1\text{H}\}$ and 2D ^1H - ^{15}N HMBC spectra were recorded on a Avance-II+ Bruker 600MHz standard bore spectrometer. A PABBO 5mm probe was manually optimized for tuning/matching to 50 Ohm on both nuclei. Solvent pre-saturation for 1s (carrier frequency set at 3.6 ppm) was applied before the acquisition of the 1D ^1H spectrum of NH_4OH (zgpr pulse program). The 1D ^{15}N - $\{^1\text{H}\}$ experiment was acquired using a simple $\pi/2$ pulse and proton decoupling during acquisition. Dioxane-d8 was used in various concentrations for deuterium lock in overnight experiments. The HMBC experiment (hmbcgpndqf pulse program) implemented gradient pulses only for coherence selection and was optimized for very weak J couplings (5 Hz). The 2D data were processed using the States reconstruction and in magnitude mode 2D representation.

CV experiments were performed with a VersaSTAT 3 Potentiostat-Galvanostat at a 100 mV/s scan rate using a 2 mm diameter Glassy Carbon disk as a working electrode, a platinum plate (6.5 x 6.5 mm square, by 0.25 mm thickness) as an auxiliary electrode, and an Ag/Ag^+ electrode composed of a silver wire immersed in acetonitrile containing 0.01 M AgNO_3 and 0.1M tetrabutylammonium perchlorate (TBAP) as a reference electrode. Concentrations and solvents for CV measurements were the same as for the model reaction with styrene **2a** (Table 1, entry 2), unless otherwise noted.

2) General procedure for the electrocatalytic aziridination

- 1) **Preparation of ammonia solution in dioxane (~ 1.5 M):** A 100 ml Schott Duran bottle was filled with 50 ml dioxane and a magnetic stir bar. After purging with N₂, ammonia gas (Ammonia N38, 99.98%, Air Liquide) was allowed to bubble through the solution while stirring until a pressure of 1.5 bar was measured. The solution was stirred for a few minutes until the ammonia pressure inside reaches an equilibrium with the solution, i.e. until a constant pressure was observed. The excess ammonia was released and the solution was quickly transferred to a 100 ml glass bottle with septum (Acros Organics AcroSeal™).

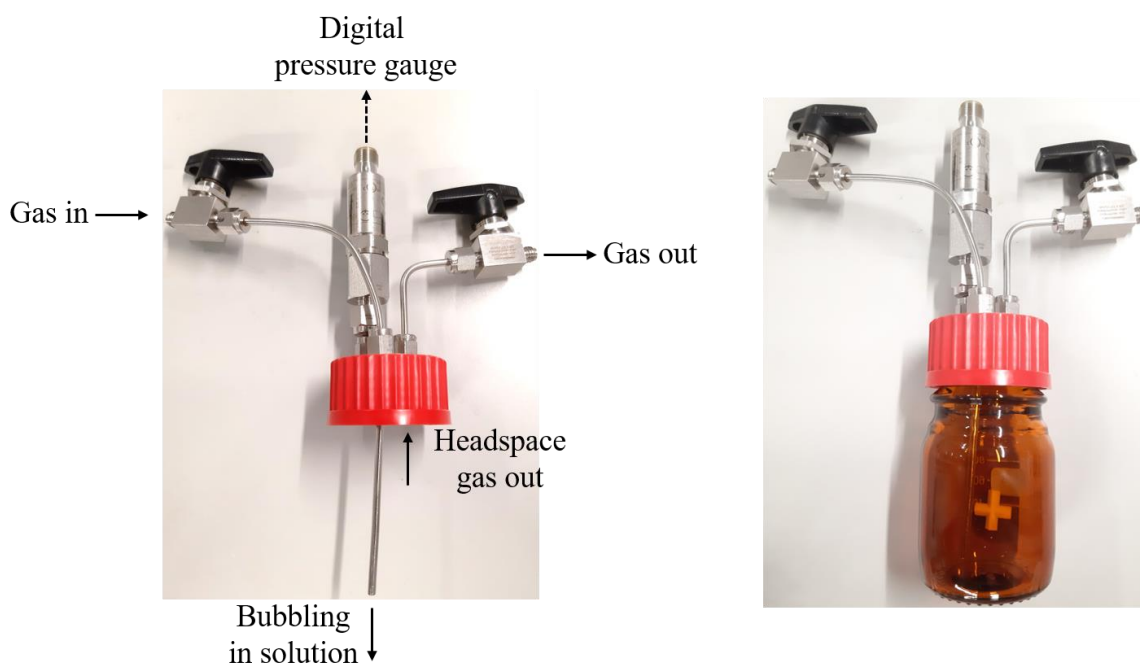


Figure S1: Set-up for the preparation of the homemade solution of ammonia in dioxane.

2) **Electrocatalytic aziridination protocol:** The glass reactor flask was charged with 0.48 mmol styrene, 5 ml homemade NH_3 solution in dioxane, 55 mg LiClO_4 , 2 equivalents of LiI , 0.6 ml H_2O and a magnetic stir bar. A carbon rod anode (6 mm ϕ , 3.5 cm long of which 2.4 cm submerged in reaction mixture) and nickel sheet cathode (1 cm wide, thickness of 0.15 mm, 3.5 cm long of which 2.4 cm submerged in reaction mixture) were attached to two stainless steel wires separated by 1 cm through a teflon support. The teflon support was inserted in the glassware causing the electrodes to be submerged in the solution, creating an undivided cell. The power supply (Tenma Bench Top Power Supply, 0-30V 3A with Single Output) was properly attached via appropriate cabling. After stirring for a few minutes to fully dissolve all the salts, a current of 40 mA was run for 3.5 hours (8.3 mA/cm^2) at room temperature. After reaction, the mixture was dried with MgSO_4 and analyzed with ^1H NMR. Pyridine was added as an external standard from a 0.045M solution in CDCl_3 . For the substrates 2- and 4-vinylpyridine (Scheme 2, entry **2o-p**), methyl 3,5-dinitrobenzoate was used as external standard. After reaction, the electrodes are washed with water and acetone. The Ni plate is scrubbed with sanding paper.

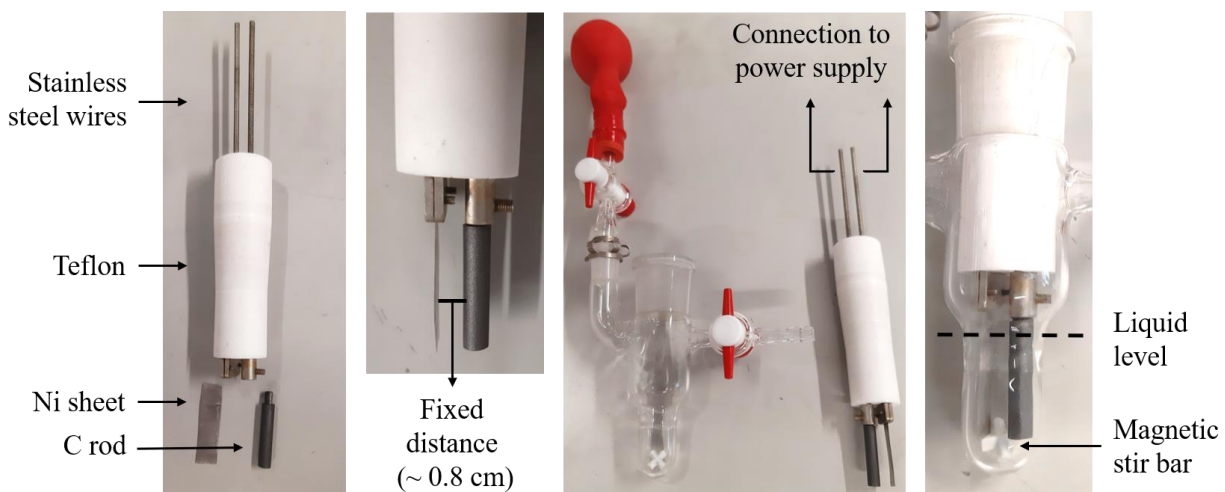


Figure S2: Electrochemical set-up.



Figure S3: Tenma Bench Top Power Supply.

- 3) **Work-up:** A work-up strategy was designed to obtain concentrated aziridines in some leftover dioxane. After performing a model reaction under standard conditions, 2 equivalents of sodium thiosulphate ($\text{Na}_2\text{S}_2\text{O}_3$) were added together with 1 ml H_2O . The resulting mixture was extracted once with excess diethyl ether (15-20 ml) and dried with MgSO_4 . Diethyl ether was removed under reduced atmosphere (rotavapor, 40 °C), together with most of the dioxane. A ^1H -NMR spectrum (CDCl_3 , no pyridine) of the model reaction mixture after work-up is included.

4) **Gram-scale experiment:** An adapted glass reactor flask was charged with 9.6 mmol styrene, 90 ml homemade NH_3 solution in dioxane (cfr. Supra), 990 mg LiClO_4 , 2 equivalents of LiI , 10 ml H_2O and a magnetic stir bar. A carbon rod anode (6 mm ϕ , 8.5 cm long of which 7.5 cm submerged in reaction mixture) and Ni sheet cathode (2 cm wide, thickness of 1 mm, 8.5 cm long of which 7.5 cm submerged in reaction mixture) were attached to a standard teflon electrode support. A current of 8.3 mA/cm^2 was run for 23 hours. After reaction, a part of the mixture was dried with MgSO_4 and analyzed with ^1H NMR. Pyridine was added as an external standard from a 0.045M solution in CDCl_3 .



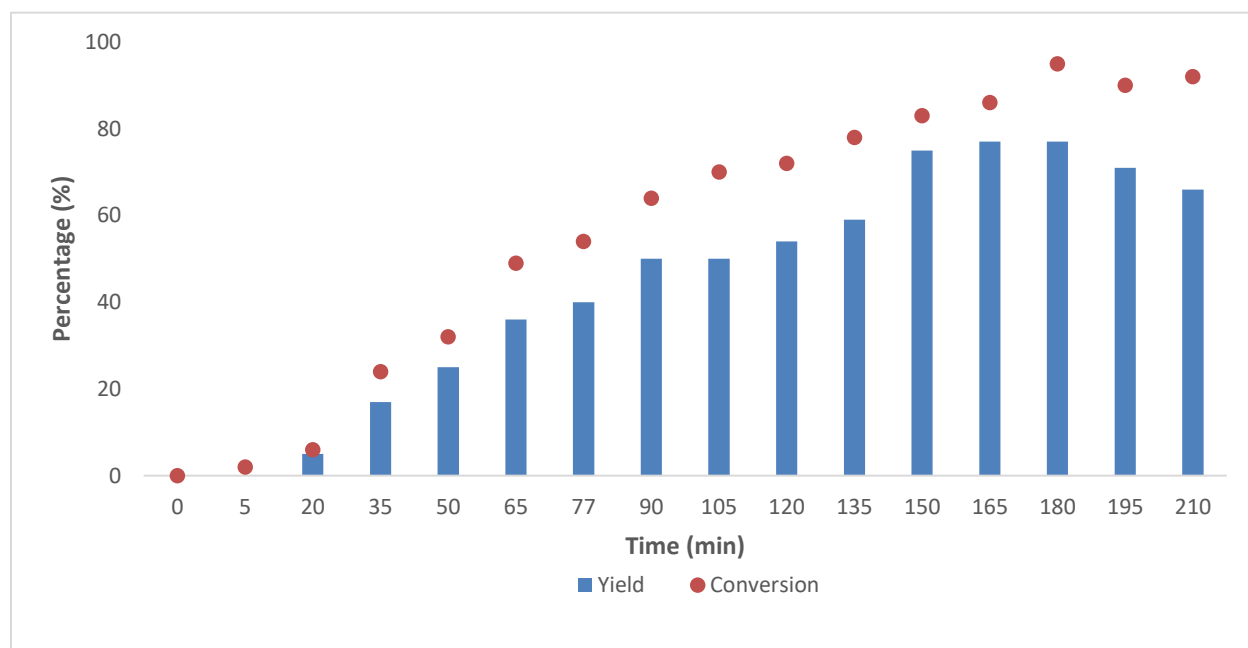
Figure S4: Electrochemical set-up for gram-scale experiment.

3) Optimization of the reaction conditions for styrene

Table S1: Optimization of catalyst, base and current

Entry	I ⁻ source	Base	Current	Yield ^a (%)
1	KI	KOtBu	40 mA	24
2	KI	KOH	40 mA	15
3	NaI	NaOtBu	40 mA	26
4	NaI	NaOH	40 mA	14
5	NaI	2,6-lutidine	40 mA	24
6	LiI	LiOtBu	40 mA	35
7	LiI	LiOH	40 mA	40
8	LiI	/	40 mA	28
9	NH ₄ I	LiOH	40 mA	28
10	TMAI	LiOH	40 mA	2
11	LiI	LiOH	20 mA	24
12	LiI	LiOH	30 mA	29
13	LiI	LiOH	50 mA	31
14	LiI	LiOH	60 mA	29
15	LiI	LiOH	70 mA	27
16	LiI	LiOH	80 mA	25
17	LiI	LiOH (0.5 equiv.)	40 mA	38
18	LiI	LiOH (2 equiv.)	40 mA	37
19	none	LiOH	40 mA	0
20	LiI (0.5 equiv)	LiOH	40 mA	17
21	LiI (2 equiv.)	none	40 mA	31
22 ^b	LiI (2 equiv.)	none	40 mA	37

Reaction conditions: 0.48 mmol styrene (**1a**), 5 ml NH₃ 0.5 M solution in dioxane, 1 equiv. I⁻ source, 1 equiv. base, 0.6 ml H₂O, Carbon rod anode 4 mm ø, Nickel sheet cathode, 4.5 F/mol. ^aGC yields of crude mixtures with ethylbenzene as external standard, percentage referring to the alkene. ^bHomemade saturated solution of ammonia in dioxane.

Table S2: Optimization of reaction time^a

Reaction conditions: 0.48 mmol styrene (**1a**), 5 ml NH₃ 0.5 M solution in dioxane, 2 equiv. LiI, 0.6 ml H₂O, Carbon rod anode 4 mm \varnothing , Nickel sheet cathode, 40 mA. ^aYields are ¹H-NMR yields (CDCl₃) of crude mixtures with pyridine as external standard, percentage referring to the alkene. Every 'timeslot' is an independent reaction.

Table S3: Solvent optimization^b

Entry	Solvent	Yield ^a (%)	Entry	Solvent	Yield ^a (%)
23	Dioxane	83	32	Propylene carbonate	< 1
24	Dimethoxy ethane	34	33	MeCN	29
25	Diglyme	13	34	DMSO	19
26	THF	< 1	35	Sulfolane	< 1
27	Me-THF	< 1	36	DMF	41
28	Cyclopentyl methyl ether	< 1	37	NMP	< 1
29	Diisopropyl ether	< 1	38	Trifluoro ethanol	< 1
30	Tert-amyl alcohol	< 1	39	HFIP	< 1
31	MeOH	13	40	EtOAc	< 1

Reaction conditions: 0.48 mmol styrene (**1a**), 5 ml NH₃ homemade solution in solvent, 0.6 ml H₂O, 2 equiv. LiI, 55 mg LiClO₄, Carbon rod anode 4 mm \varnothing , Nickel sheet cathode, custom teflon electrode support, 40 mA, 210 minutes. Crude mixtures were dried with MgSO₄ before analysis. ^aYields are ¹H-NMR yields (CDCl₃) of crude mixtures with pyridine as external standard, percentage referring to the alkene. ^bAdditionally, different ratios of dioxane/H₂O, dioxane/MeOH and MeCN/H₂O were tested but did not provide any improvement.

Table S4: Final optimizations

Entry	Deviation	55 mg LiClO ₄	Time (min)	Yield ^a (%) ^b
41	-	-	150	76
42	-	yes	150	75 (99)
43	Carbon anode 6 mm ø	-	150	76
44	-	-	180	81
45	-	yes	180	81
46	-	yes	210	83
47	-	yes	240	85
48	-	yes	270	84
49	Carbon anode 6 mm ø	yes	210	94 (99)
50	LiI 3 equiv.	yes	210	88
51	LiI 3 equiv.	yes	270	89
52	70 mA, 120 min	yes	210	78
53	100 mA, 84 min	yes	210	79
54	Styrene 0.96 mmol	yes	210	68
55 ^c	LiI 1 equiv.	Yes	210	62
56 ^c	LiI 0.5 equiv.	Yes	210	30
57 ^c	Li 1 equiv.	Yes, 110 mg	210	37
58	Carbon anode 6 mm ø	Yes, 110 mg	180	71
59 ^c	NaI 2 equiv.	Yes	210	49
60 ^c	KI 2 equiv.	Yes	210	67
61 ^c	NH ₄ I 2 equiv.	Yes	210	3
62 ^c	NH ₄ I 1 equiv.	Yes	210	29

Reaction conditions: 0.48 mmol styrene (**1a**), 5 ml NH₃ homemade solution in dioxane (~1.5 M), 2 equiv. LiI, 0.6 ml H₂O, Carbon rod anode 4 mm ø, Nickel sheet cathode, custom teflon electrode support, 40 mA. Crude mixtures were dried with MgSO₄ before analysis. ^aYields are ¹H-NMR yields (CDCl₃) of crude mixtures with pyridine as external standard, percentage referring to the alkene. ^bSelectivity in parentheses. ^cCarbon rod anode 6 mm ø (with 40 mA of current, this corresponds to 8.3 mA/cm².)

4) Calculating the Faradaic efficiency; experiments in a divided cell

The Faradaic efficiency FE is calculated as follows:

$$FE = \frac{n_S * n_e * F}{I * t} * Y_S \quad \text{Eq. S1}$$

Where n_S stands for the number of moles of substrate S, n_e for the number of electrons necessary for the envisioned reaction for each molecule (2 for the aziridination), F for Faraday's constant (96485 C mol⁻¹), I for the current in Ampère, t for the time in seconds and Y_S for the yield of the product. For the model reaction system using styrene (Table 1, entry 2 in the manuscript), the FE is equal to 17.3%. With double the amount of styrene added (Table S4, entry 54), a yield of 68% was achieved with the same reaction time, which corresponds to an FE = 25.0%. With an hour less reaction time but still an acceptable yield of 75% (Table S4, entry 42), the FE = 19.3%. With 4-methoxystyrene as the substrate, a yield of 70% was obtained while the reaction time was halved. This corresponds to an FE = 25.7%.

We expect, besides additional H₂ production, that anodically generated species are reduced again at the cathode (for instance I₂) resulting in a net zero reaction while electricity is consumed. Therefore, we explored the use of a divided cell in an attempt to increase the Faradaic efficiency (Figure S5).

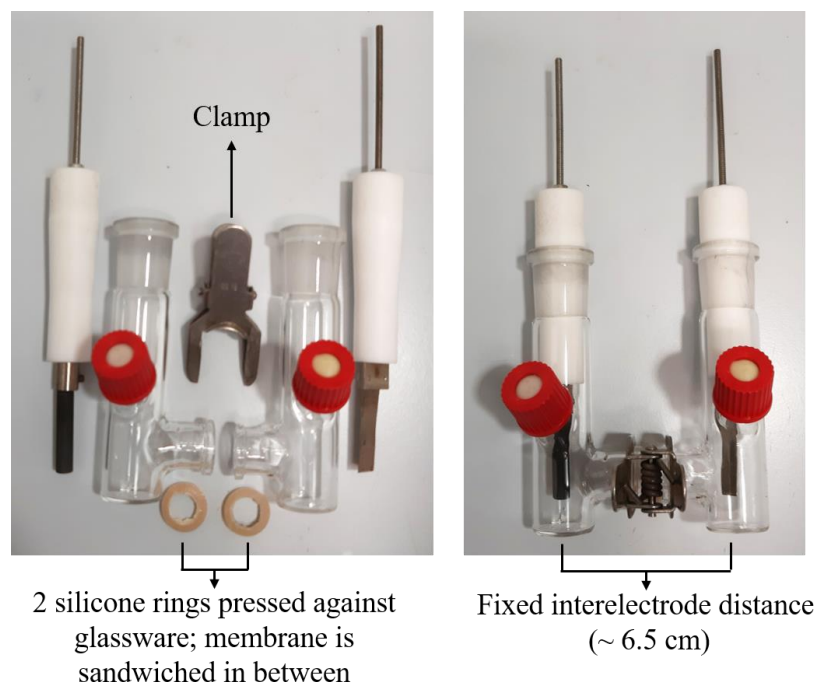


Figure S5: Electrochemical divided cell set-up.

The divided cell required twice the volume in each compartment in order to fully cover the membrane. In the anodic compartment, similar equivalents of reagents and solvents were used as for the optimized reaction system in the undivided cell (see Manuscript Table 1, entry 2). For the cathodic compartment, only water is used with equal amounts of LiClO_4 as in the anodic compartment. Since the interelectrode distance is increased by a factor of ~ 8 , a membrane separates the 2 compartments and dioxane is poorly conducting (even with the additional water) the voltage was too high in order to support a current of 40 mA as reported for the standard conditions. Therefore a current of 10 mA was used. As a consequence, longer reaction times were needed, also due to the fact that a double amount of styrene was used, even when a charge consumption of only 2.3 F/mol (355 minutes) was used. Several adaptations to the conditions were tested:

Table S5: Divided cell

Entry	Deviation	Time (min)	Charge (F/mol)	Yield (%) ^a	FE (%)
63	-	355	2.3	22	19.1
64	Nafion (115) membrane	355	2.3	18	15.7
65	LiOH 1 equiv. in anod. comp.	355	2.3	21	18.3
66 ^b	0.48 mmol styrene	230	3	trace	< 1
67 ^b	1.92 mmol styrene	1235	4	52	26.0
68	1.2 ml NH ₄ OH in cathod. comp.	1080	7	60	17.2
69	-	1080	7	62	17.7

Standard conditions: Anodic compartment: 0.96 mmol styrene (**1a**), 10 ml NH₃ homemade solution in dioxane (~1.5 M), 2 equiv. LiI, 2 equiv. LiClO₄, 1.2 ml H₂O, Carbon rod anode 6 mm ϕ . Cathodic compartment: 11.2 ml H₂O, 2 equiv. LiClO₄, Ni sheet cathode. AMI-7001 membrane. Custom teflon electrode supports, 10 mA. Crude mixtures were dried with MgSO₄ before analysis. ^aYields are ¹H-NMR yields (CDCl₃) of crude mixtures with pyridine as external standard, percentage referring to the alkene. ^bAmounts of LiI and LiClO₄ were kept the same as for the standard conditions, only amounts of styrene were altered.

No real improvement in the Faradaic efficiency could be made. A value of 26% is within experimental error of the values of 25.7% and 25% with other entries (see above).

5) Spectrophotometry

We measured the absorption spectra for 3 different solutions in the range of 250-800 nm; A) the model reaction system (with all reactants as described by the standard conditions in the manuscript) in the absence of styrene, applying a current of 40 mA for 210 minutes, B) the model reaction system in the absence of styrene, but without current, and C) the model reaction system without both styrene and applied current and where the 2 equivalents of LiI were replaced with I₂. Two absorption bands (292 nm and 362 nm) can clearly be seen for solutions A and C, which correspond nicely to triiodide¹⁻². No spectrophotometrical evidence was found for other species.

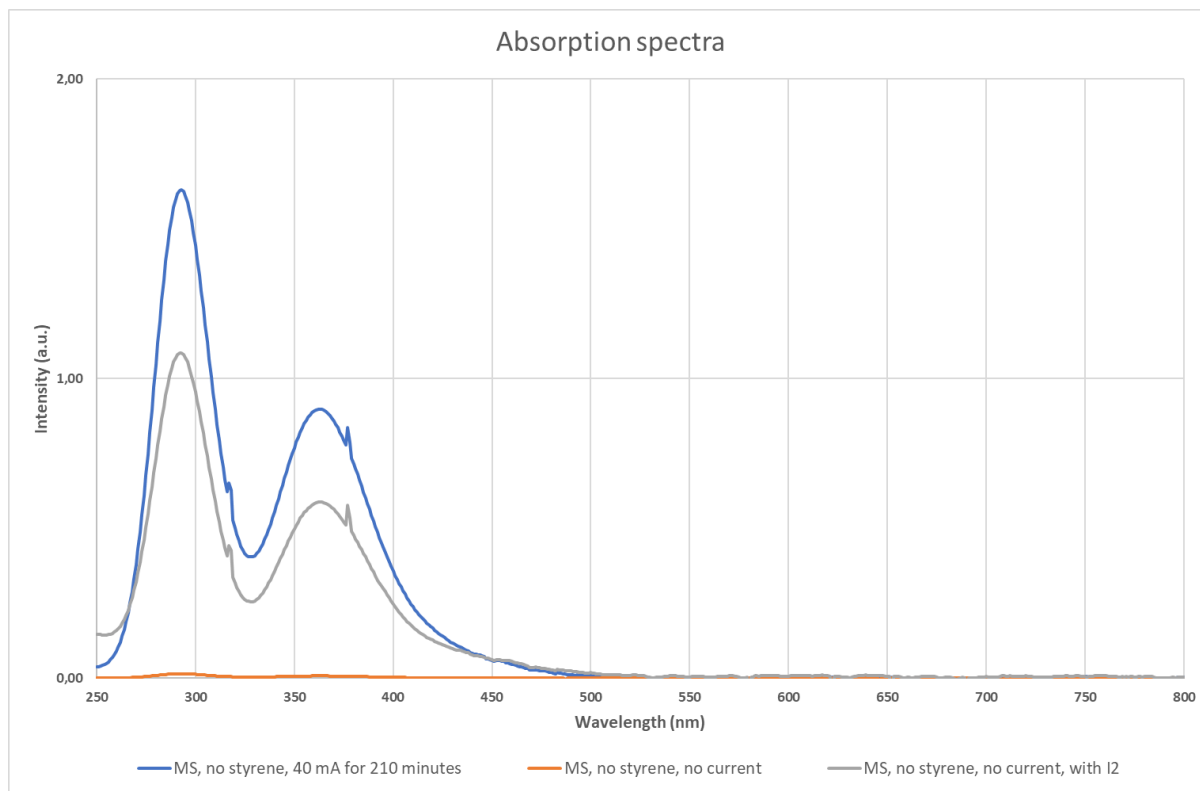


Figure S6: Absorption spectra of several combinations of the different reactants. MS = model reaction system in standard conditions as mentioned in the manuscript (Table 1), consisting of styrene, dioxane, water, LiI, LiClO₄, and ammonia.

6) Cyclic Voltammetry experiments

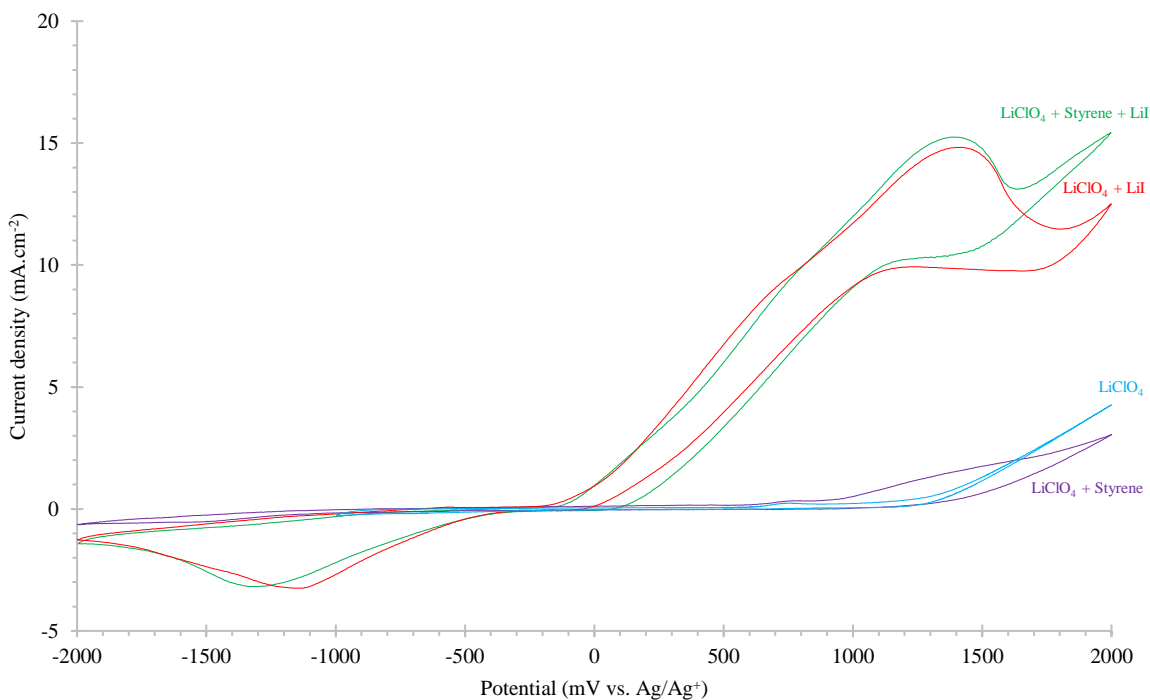


Figure S7: CV analysis on various combinations of reactants in systems without ammonia.

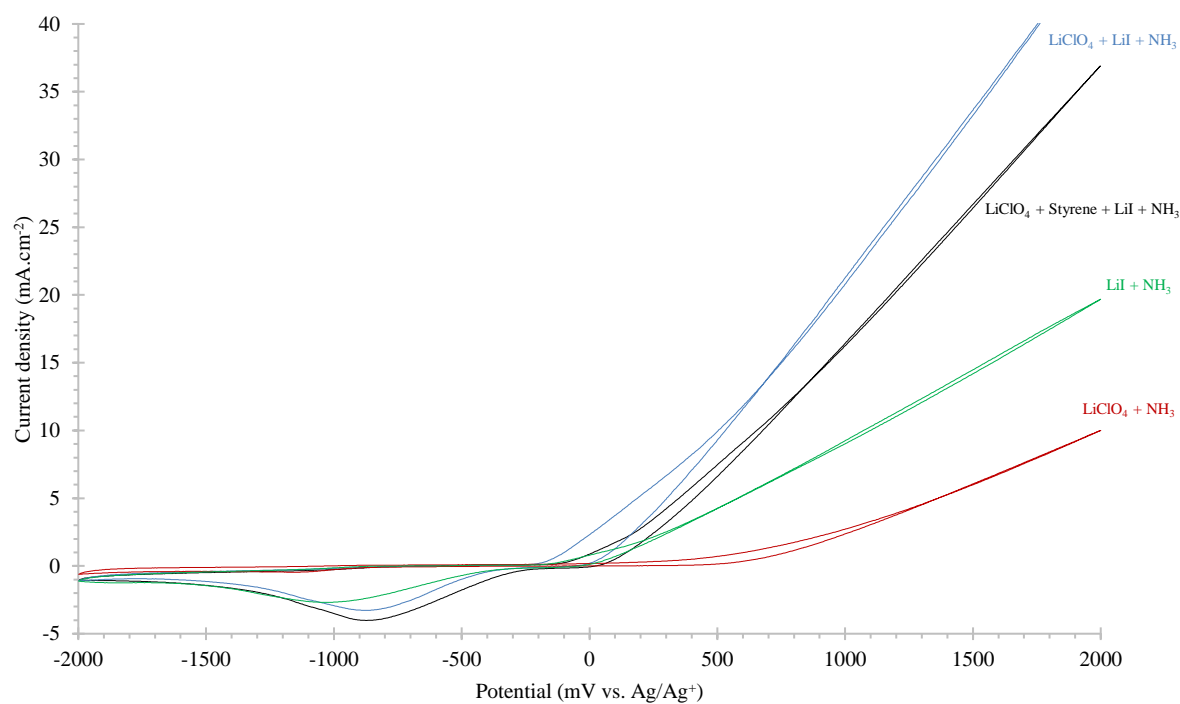


Figure S8: CV analysis on various combinations of reactants in ammonia containing systems.

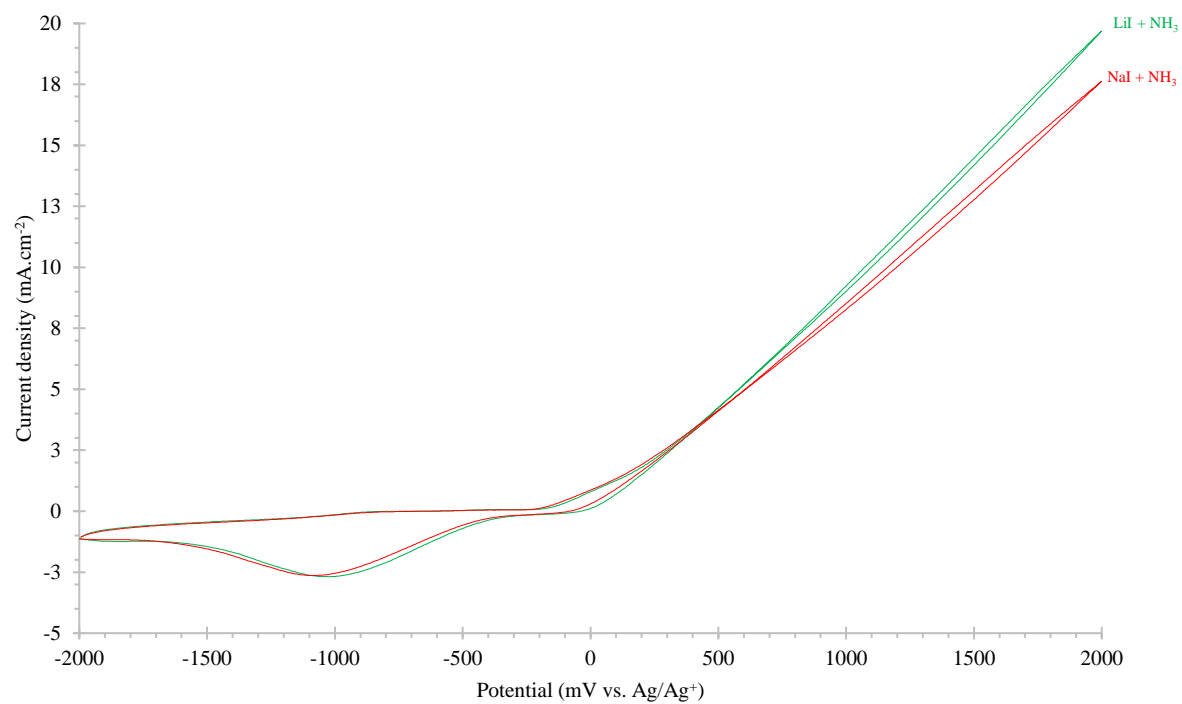


Figure S9: CV analysis comparing NaI and LiI behavior in the model reaction system containing ammonia.

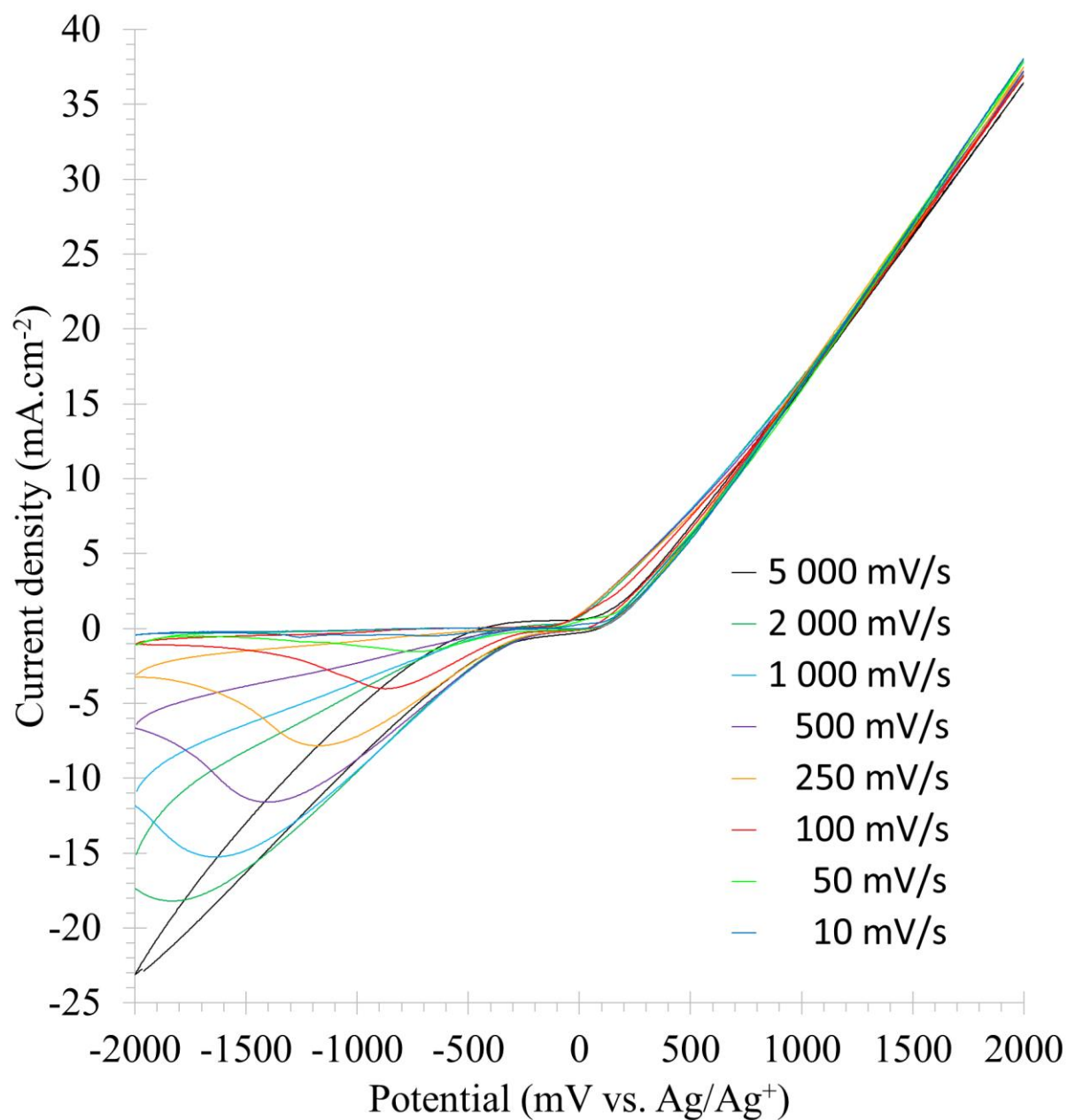


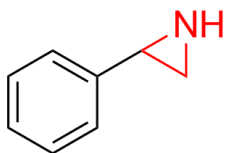
Figure S10: CV analysis comparing the behavior of the model reaction system containing ammonia with different scan rates. A clear variation with the scan rate is visible for the cathodic current. This can be related to the gradual consumption of I^+ species in a consecutive reaction with NH_3 .

7) Spectroscopic data

Quantification was performed using 200 μl of crude reaction mixture with 300 μl 0.0454 M solution of pyridine in CDCl_3 . Characteristic signals of both starting materials and products, together with the signal for pyridine at $\delta = 8.58$ (d, 2H), are used. For the model reaction with styrene (**2a**), quantification was based on the styrene signal at $\delta = 5.74$ (d, 1H) and the aziridine signal at $\delta = 2.18$ (d, 1H). Similar strategies were used for the other substrates. For vinylpyridine substrates **2t-u**, a 0.0214 M solution of methyl 3,5-dinitrobenzoate in CDCl_3 was used with a characteristic signal $\delta = 9.11$ (s, 2H).

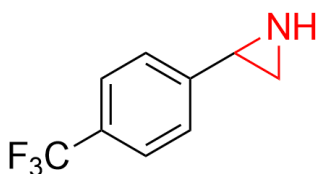
The crude spectra for quantification were compared with literature data to prove the aziridine had formed³⁻⁷. However, no distinctive peak of the N-H proton could be discriminated from other signals, most likely because it is an exchangeable proton and due to H-bonding with both dioxane and especially water, broadening and displacing the peak. According to literature, this proton gives a broad signal around $\delta = 0.81$, but also $\delta = 1.51$ is reported⁸. After work-up, the N-H proton signal was found at $\delta = 1.32$. However, H-bonding with leftover dioxane can still be responsible for broadening and displacing the signal. GC-MS measurements and ^{15}N -NMR measurements further confirmed the aziridine formation.

2-phenylaziridine (2a)



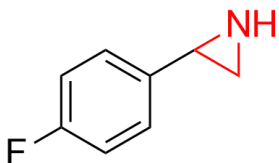
$^1\text{H-NMR}$ (300 MHz, CDCl_3) δ 1.26 (s br, 1H), 1.79 (d, 1H), 2.18 (d, 1H), 3.00 (dd, 1H), 7.17 – 7.36 (m, 5H); $^{13}\text{C-NMR}$ (300 MHz, CDCl_3) δ 140.6, 128.1, 126.9, 125.9, 31.9, 29.4; GC-MS (EI, 70eV): m/z (rel. int. %): 119 (14), 118 (100), 117 (14), 92 (5), 91 (28), 90 (5), 89 (12), 77 (6), 65 (7), 63 (9), 51 (6), 50 (5), 39 (6), 32 (8)

2-(4-trifluoromethylphenyl)-aziridine (2b)



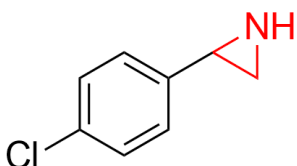
$^1\text{H-NMR}$ (300 MHz, CDCl_3) δ 1.26 (s br, 1H), 1.70 (d, 1H), 2.25 (d, 1H), 3.07 (dd, 1H), 7.37 (d, 2H), 7.55 (d, 2H)

2-(4-fluorophenyl)-aziridine (2c)



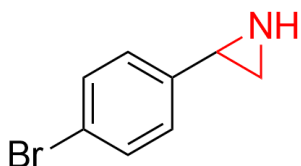
$^1\text{H-NMR}$ (300 MHz, CDCl_3) δ 1.26 (s br, 1H), 1.72 (d, 1H), 2.18 (d, 1H), 3.00 (dd, 1H), 7.00 (d, 2H), 7.31 (d, 2H)

2-(4-chlorophenyl)-aziridine (2d)



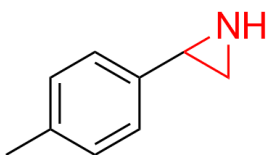
$^1\text{H-NMR}$ (300 MHz, CDCl_3) δ 1.26 (s br, 1H), 1.70 (d, 1H), 2.19 (d, 1H), 2.98 (dd, 1H), 7.14 – 7.36 (m, 4H)

2-(4-bromophenyl)-aziridine (2e)



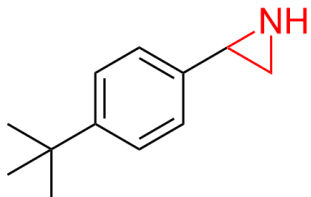
$^1\text{H-NMR}$ (300 MHz, CDCl_3) δ 1.26 (s br, 1H), 1.69 (d, 1H), 2.19 (d, 1H), 2.97 (dd, 1H), 7.12 (d, 2H), 7.42 (d, 2H)

2-(4-methylphenyl)-aziridine (2f)



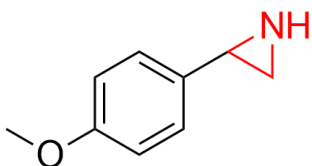
$^1\text{H-NMR}$ (300 MHz, CDCl_3) δ 1.26 (s br, 1H), 1.85 (d, 1H), 2.16 (d, 1H), 2.31 (s, 3H), 2.98 (dd, 1H), 7.04 – 7.16 (m, 4H)

2-(4-*tert*-butylphenyl)-aziridine (2g)



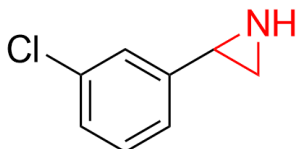
$^1\text{H-NMR}$ (300 MHz, CDCl_3) δ 1.26 (s br, 1H), 1.30 (s, 9H), 1.85 (d, 1H), 2.16 (s, 1H), 2.98 (dd, 1H), 7.24 – 7.39 (m, 4H)

2-(4-methoxyphenyl)-aziridine (2h)



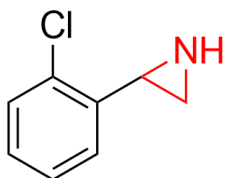
$^1\text{H-NMR}$ (300 MHz, CDCl_3) δ 1.26 (s br, 1H), 1.69 (d, 1H), 2.11 (d, 1H), 2.93 (dd, 1H), 3.84 (s, 3H), 6.89 (d, 2H), 7.38 (d, 2H)

2-(3-chlorophenyl)-aziridine (2i)



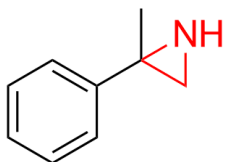
$^1\text{H-NMR}$ (300 MHz, CDCl_3) δ 1.26 (s br, 1H), 1.67 (d, 1H), 2.18 (d, 1H), 2.97 (dd, 1H), 7.10 – 7.34 (m, 4H)

2-(2-chlorophenyl)-aziridine (2j)



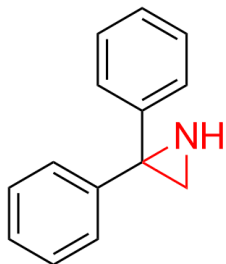
$^1\text{H-NMR}$ (300 MHz, CDCl_3) δ 1.26 (s br, 1H), 1.61 (d, 1H), 2.26 (d, 1H), 3.32 (dd, 1H), 7.16 – 7.36 (m, 3H), 7.58 (d, 1H)

2-methyl-2-phenylaziridine (2k)



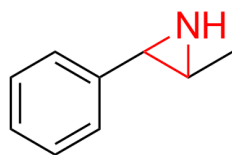
$^1\text{H-NMR}$ (300 MHz, CDCl_3) δ 1.26 (s br, 1H), 1.60 (s, 3H), 1.96 (d, 2H), 7.17 – 7.38 (m, 5H)

2,2-diphenylaziridine (2l)



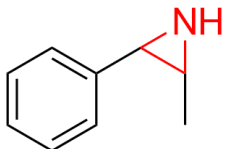
$^1\text{H-NMR}$ (300 MHz, CDCl_3) δ 1.26 (s br, 1H), 2.34 (s, 2H), 7.17 – 7.39 (m, 10H)

***trans*-2-methyl-3-phenylaziridine (2ma)**



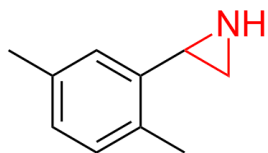
$^1\text{H-NMR}$ (300 MHz, CDCl_3) δ 1.26 (s br, 1H), 1.33 (d, 3H), 2.13 (m, 1H), 2.63 (d, 1H), 7.11 – 7.34 (m, 5H)

***cis*-2-methyl-3-phenylaziridine (2mb)**



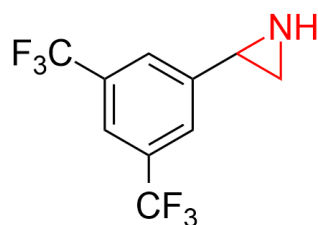
$^1\text{H-NMR}$ (300 MHz, CDCl_3) δ 0.88 (d, 3H), 1.26 (s br, 1H), 2.38 (m, 1H), 3.21 (d, 1H), 7.11 – 7.34 (m, 5H)

2-(2,5-dimethylphenyl)-aziridine (2p)



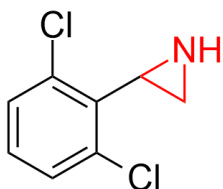
$^1\text{H-NMR}$ (300 MHz, CDCl_3) δ 1.26 (s br, 1H), 1.66 (d, 1H), 2.31 (d, 1H), 3.17 (dd, 1H), 7.61 – 7.90 (m, 3H)

2-(3,5-bis(trifluoromethyl)phenyl)-aziridine (2q)



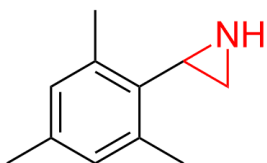
$^1\text{H-NMR}$ (300 MHz, CDCl_3) δ 1.26 (s br, 1H), 1.67 (d, 1H), 2.30 (d, 1H), 3.15 (dd, 1H), 7.63 – 7.91 (m, 3H)

2-(2,6-dichlorophenyl)-aziridine (2r)



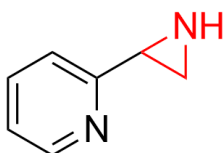
$^1\text{H-NMR}$ (300 MHz, CDCl_3) δ 1.26 (s br, 1H), 1.98 (d, 1H), 2.33 (d, 1H), 3.00 (dd, 1H), 7.06 – 7.38 (m, 3H)

2-(2,4,6-trimethylphenyl)-aziridine (2s)



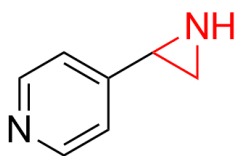
$^1\text{H-NMR}$ (300 MHz, CDCl_3) δ 1.26 (s br, 1H), 1.76 (d, 1H), 2.15 (d, 1H), 2.37 (s, 6H), 2.91 (dd, 1H), 6.73 – 6.88 (m, 2H)

2-(2-aziridiny)-pyridine (2t)



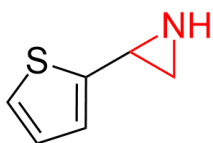
$^1\text{H-NMR}$ (300 MHz, CDCl_3) δ 1.26 (s br, 1H), 2.00 (d, 1H), 2.07 (d, 1H), 3.03 (dd, 1H), 7.16 (m, 1H), 7.36 (d, 1H), 7.64 (m, 1H), 8.56 (d, 1H)

4-(2-aziridiny)-pyridine (2u)



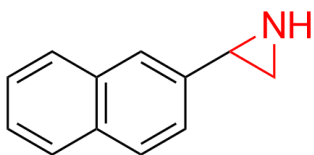
$^1\text{H-NMR}$ (300 MHz, CDCl_3) δ 1.26 (s br, 1H), 1.71 (d, 1H), 2.28 (d, 1H), 2.99 (dd, 1H), 7.31 (d, 2H), 8.52 (d, 2H)

2-(2-thienyl)-aziridine (2v)



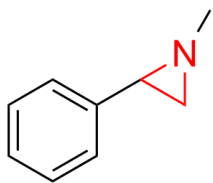
$^1\text{H-NMR}$ (300 MHz, CDCl_3) δ 1.26 (s br, 1H), 1.94 (d, 1H), 2.18 (d, 1H), 3.20 (dd, 1H), 6.96 (m, 2H), 7.18 (m, 1H)

2-(2-naphthalenyl)-aziridine (2w)



$^1\text{H-NMR}$ (300 MHz, CDCl_3) δ 1.26 (s br, 1H), 1.91 (d, 1H), 2.26 (d, 1H), 3.17 (dd, 1H), 7.26 – 7.34 (m, 2H), 7.38 – 7.48 (m, 1H), 7.66 – 7.82 (m, 4H)

1-methyl-2-phenylaziridine (2x)



$^1\text{H-NMR}$ (300 MHz, CDCl_3) δ 1.65 (d, 1H), 1.93 (d, 1H), 2.29 (dd, 1H), 2.51 (s, 3H), 7.22 – 7.48 (m, 5H)

^1H -NMR spectrum of the model reaction mixture after removal of electrolytes and solvent.

Leftover styrene (characteristic signals between 5.2 and 6.8 ppm) and dioxane (3.7 ppm) are also visible.

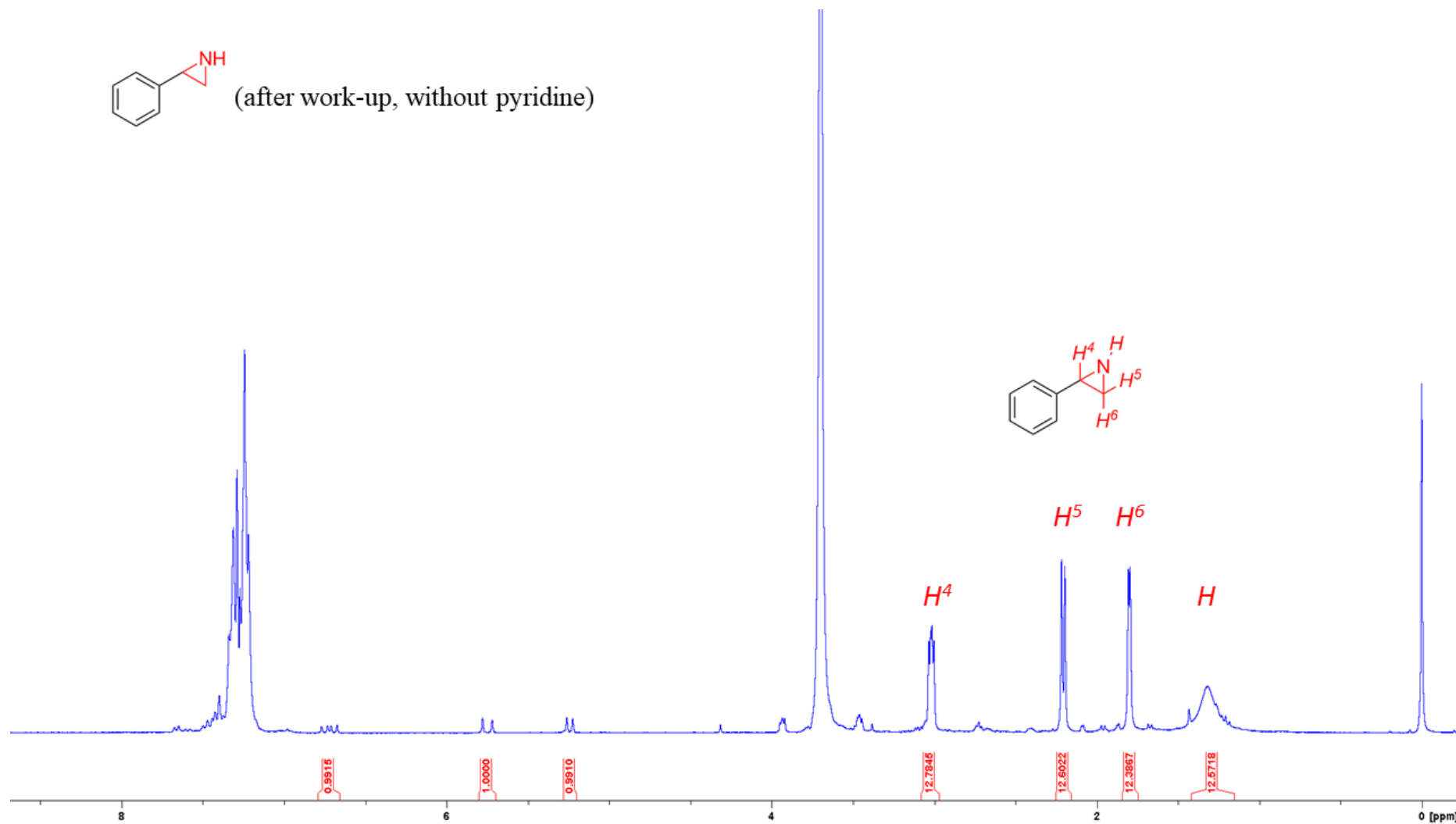


Figure S11: ^1H -NMR spectrum of the model reaction mixture after removal of electrolytes and solvent.

^{15}N -NMR spectrum of the model reaction with styrene performed with $^{15}\text{NH}_4\text{OH}$.

Ammonia is set as a reference at 0 ppm. The 2-phenylaziridine signal is clearly visible at 16 ppm, while 2 other signals at 103 and 256 ppm can be seen. Spectrum part of an overnight measurement.

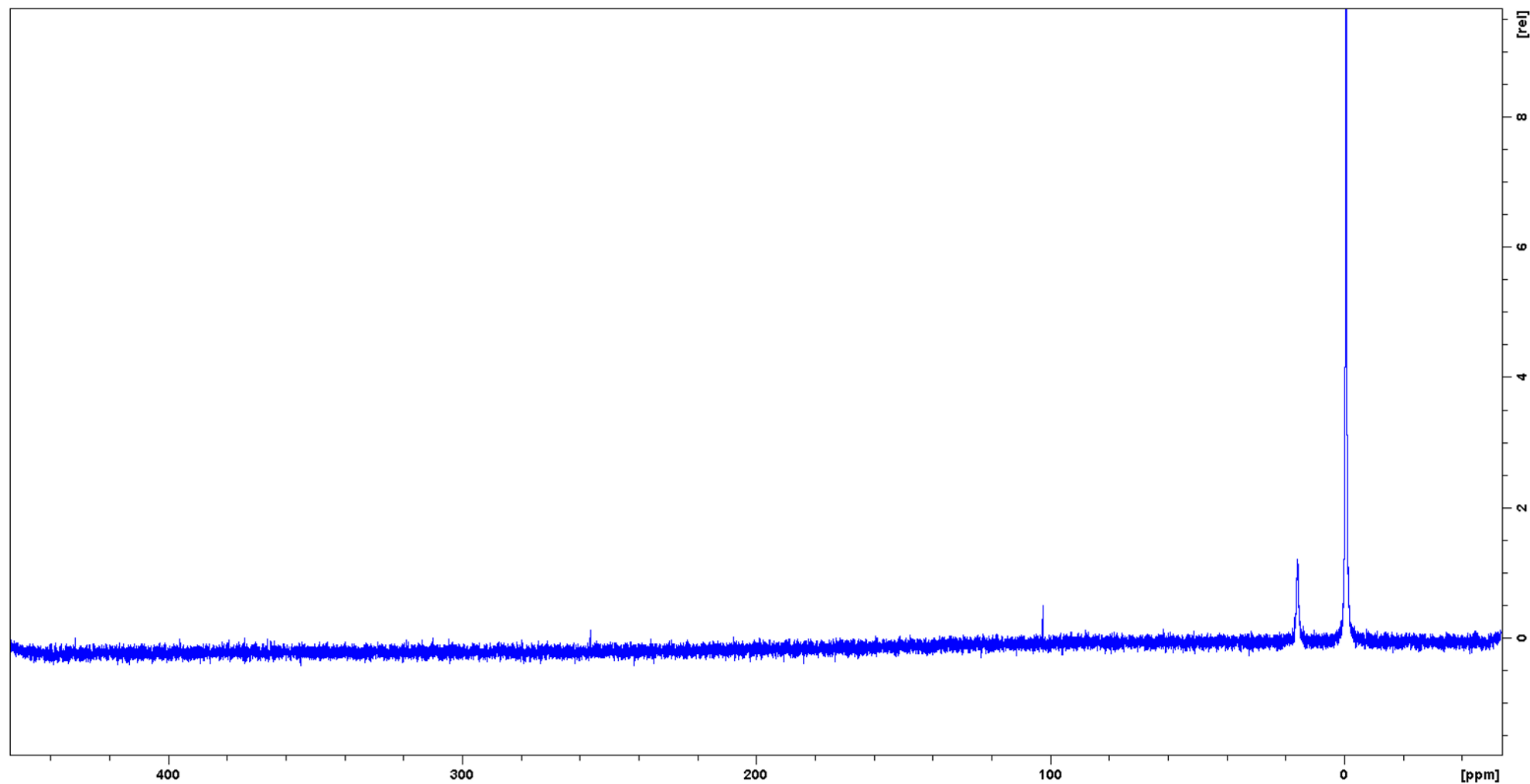


Figure S12: ^{15}N -NMR spectrum of the model reaction with styrene performed with $^{15}\text{NH}_4\text{OH}$, according to the conditions of Table 1, entry 12 of the manuscript.

^{15}N -NMR spectrum after work-up of the model reaction with styrene performed with $^{15}\text{NH}_4\text{OH}$.

Only the signal of 2-phenylaziridine remains visible.

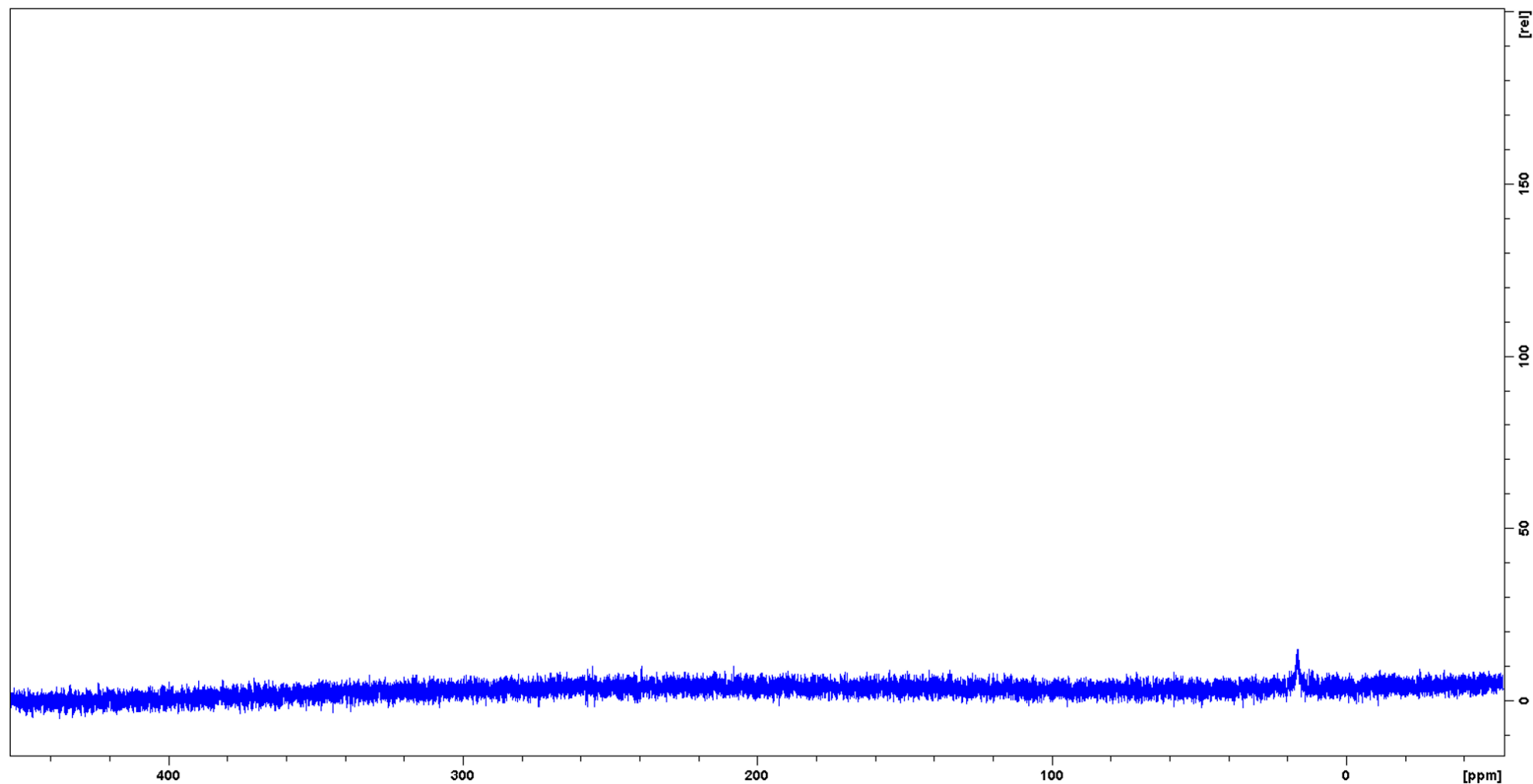


Figure S13: ^{15}N -NMR spectrum after work-up of the model reaction with styrene performed with $^{15}\text{NH}_4\text{OH}$, according to the conditions of Table 1, entry 12 of the manuscript.

^1H -NMR spectrum of $^{15}\text{NH}_4\text{OH}$ with solvent pre-saturation directly from the commercial bottle.

Some impurities are clearly visible

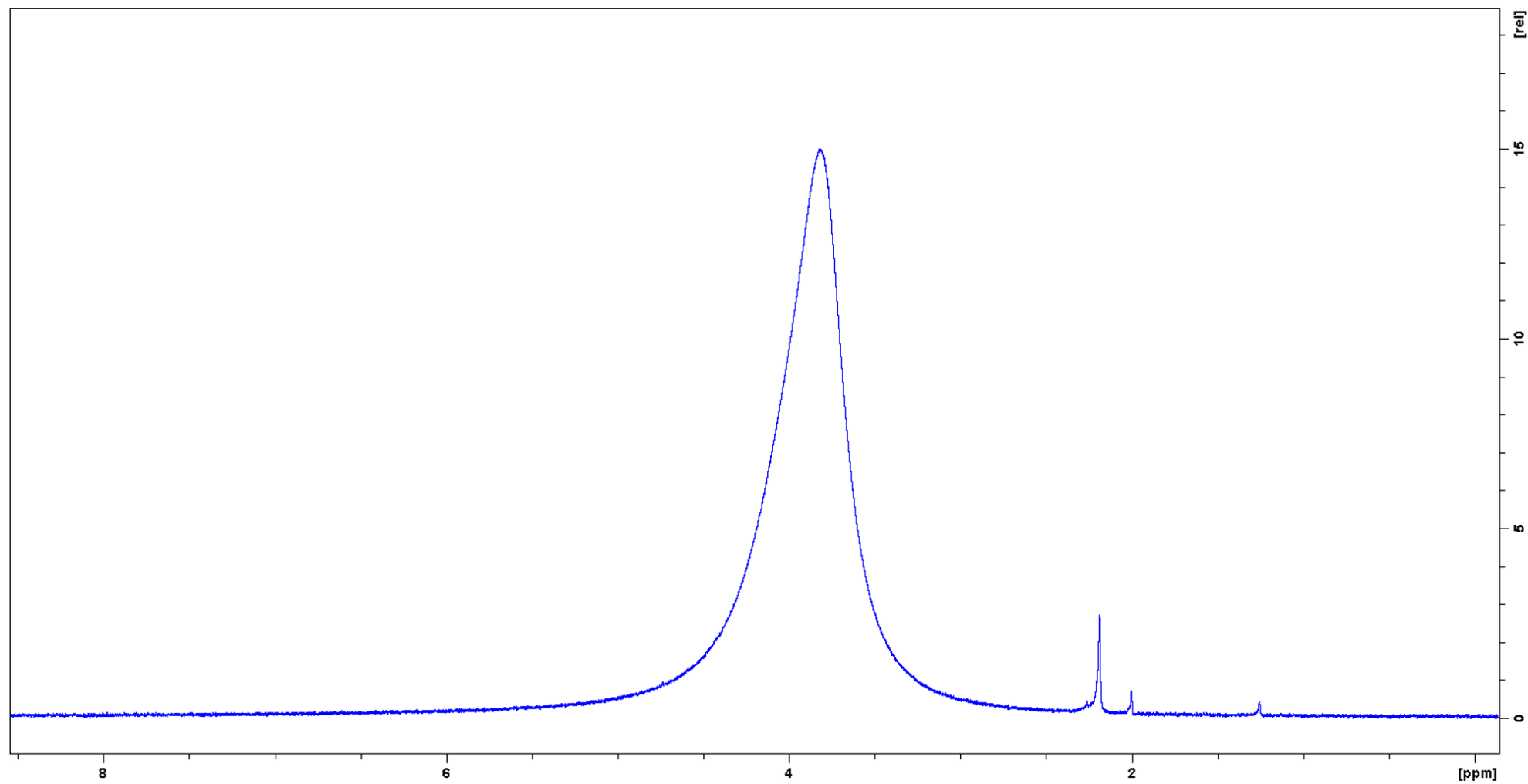


Figure S14: ^1H -NMR spectrum of $^{15}\text{NH}_4\text{OH}$ with solvent pre-saturation directly from the commercial bottle.

^1H - ^{15}N HMBC spectrum of the model reaction mixture with styrene performed with $^{15}\text{NH}_4\text{OH}$

Impurities from the $^{15}\text{NH}_4\text{OH}$ bottle are also visible here with a different chemical shift in ^{15}N (106 and 245 ppm). The signal for $^{15}\text{NH}_3$ is now located underneath the large vertical band created due to residual proton signal from the dioxane solvent. The extra signals seen in the ^{15}N -NMR spectrum at 103 and 256 ppm (see above) correspond to signals at 3.95 and 4.37 ppm in ^1H respectively. The 3 signals at 16 ppm in ^{15}N correspond to 2-phenylaziridine.

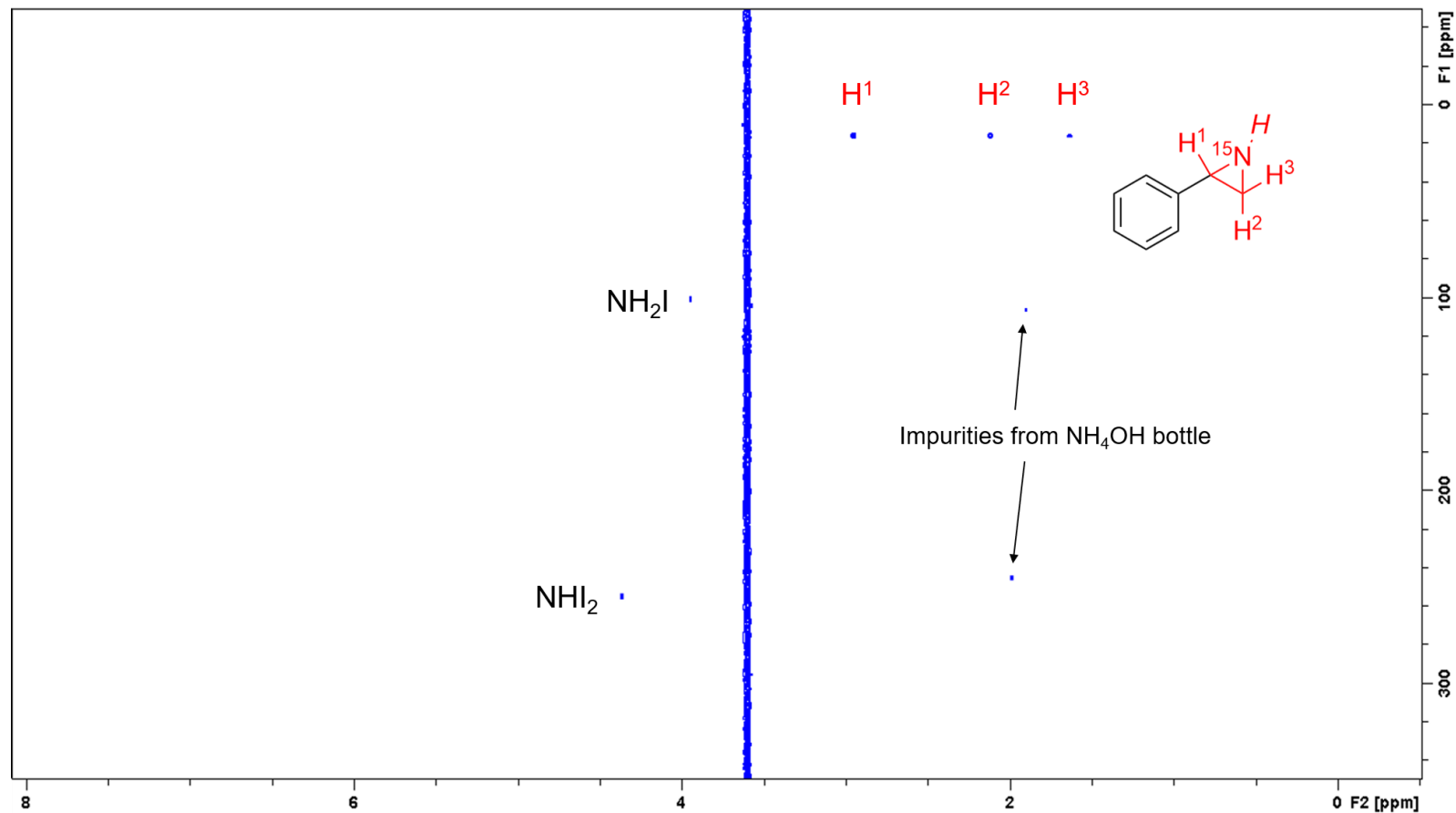


Figure S15: ^1H - ^{15}N HMBC spectrum of the model reaction mixture with styrene performed with $^{15}\text{NH}_4\text{OH}$.

^1H - ^{15}N HMBC spectrum of the model reaction mixture without styrene performed with $^{15}\text{NH}_4\text{OH}$

The same signals as above, except for the ones arising from 2-phenylaziridine, are found when the reaction is carried out without styrene. This is an additional indication that indeed NH_2I and NHI_2 are formed. An extra signal (doublet) in ^1H dimension, corresponding to a singlet in ^{15}N dimension, is observed.

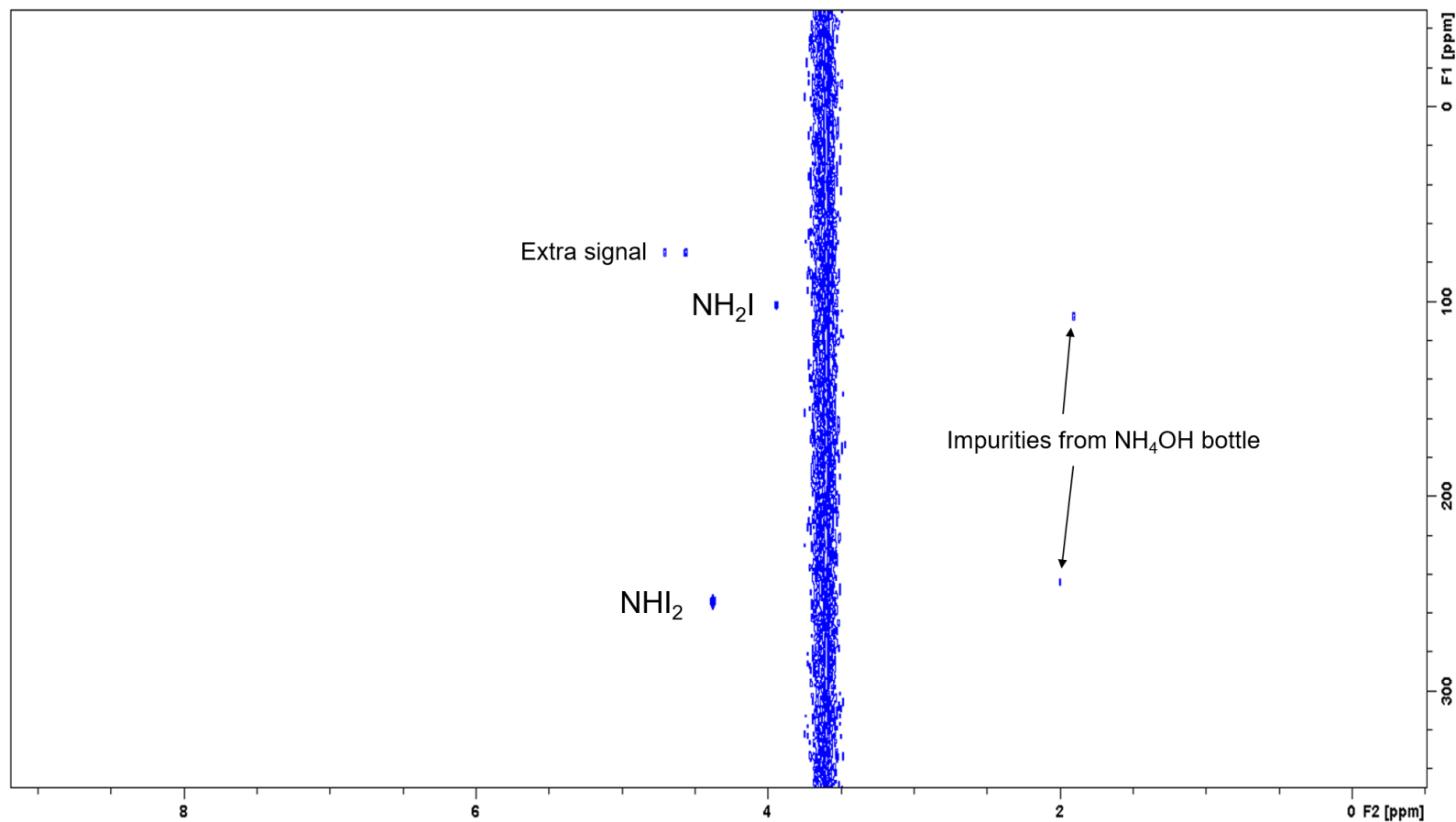


Figure S16: ^1H - ^{15}N HMBC spectrum of the model reaction mixture without styrene performed with $^{15}\text{NH}_4\text{OH}$.

^1H -NMR spectrum of a model reaction without styrene ($^{14}\text{NH}_3$ solution in dioxane) with solvent suppression after addition of 2 drops of sulfuric acid (96%)

In literature it is known that addition of an acid to $^{14}\text{NH}_3$ -containing systems ($I = 1$) can impede the fast exchange of protons, resulting in splitting of the singlet signal into a 1-1-1 triplet signal⁹⁻¹⁰. Unfortunately, only one such triplet was observed when a small amount of sulfuric acid was added to an analogous mixture prepared with $^{14}\text{NH}_3$ which is most likely originating from NH_4^+ . No other triplet signal was observed which might have come from NH_3I^+ . This is ascribed to a shift of the equilibrium between I_2 and NH_3 (like C' in Scheme 3) due to removal of NH_3 to NH_4^+ and the stronger acidity of NH_3I^+ compared to that of NH_4^+ .

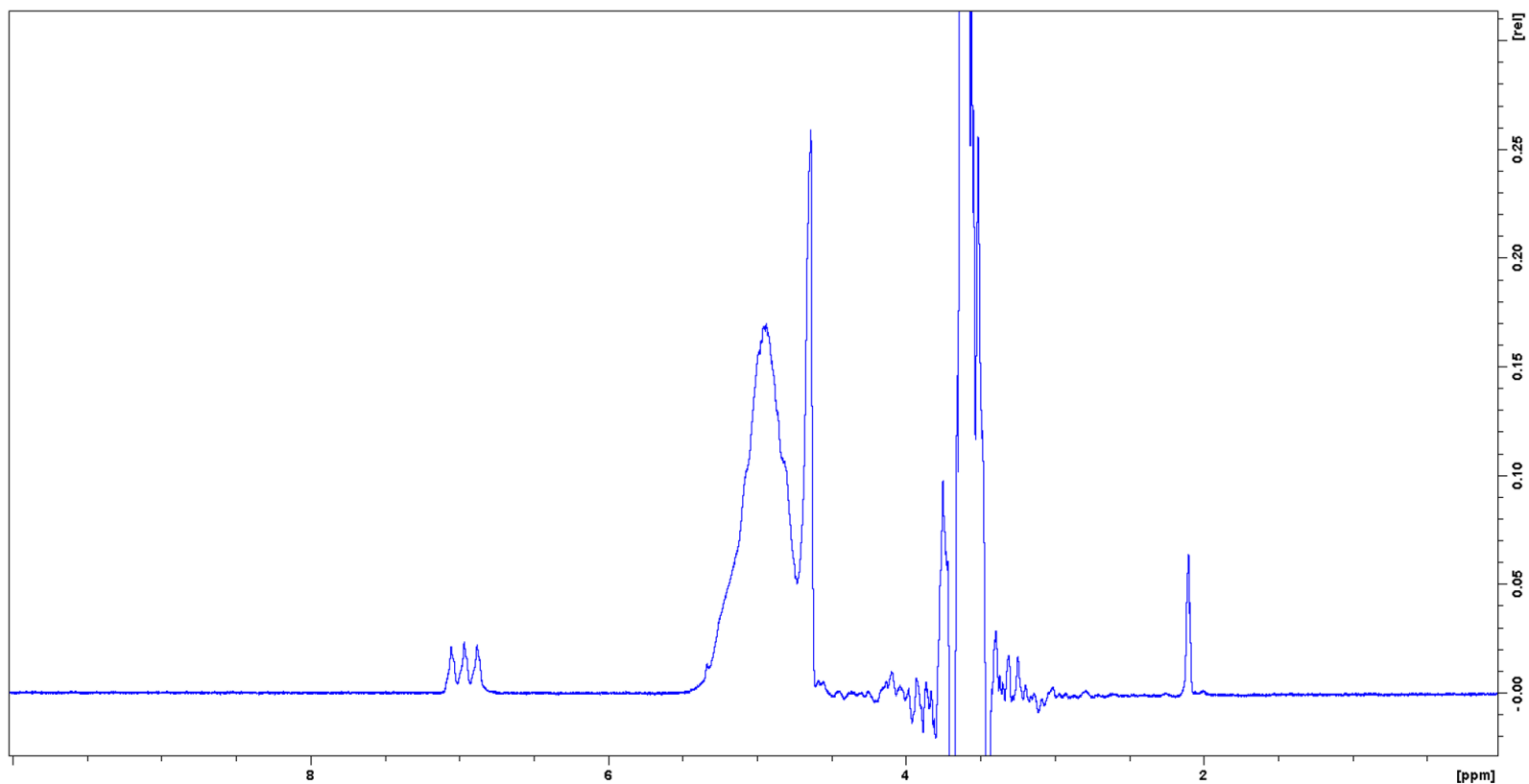


Figure S17: ^1H -NMR spectrum of a model reaction without styrene ($^{14}\text{NH}_3$ solution in dioxane) with solvent suppression after addition of 2 drops of sulfuric acid (96%).

8) References

- (1) Jung, S.-H.; Yeon, J.-W.; Kang, Y.; Song, K. Determination of Triiodide Ion Concentration Using UV Visible Spectrophotometry. *Asian J. Chem.* **2014**, 26, 4084-4086, DOI 10.14233/ajchem.2014.17720.
- (2) Awtrey, A. D.; Connick, R. E. The Absorption Spectra of I_2 , I_3^- , I^- , IO_3^- , $S_4O_6^{2-}$ and $S_2O_3^{2-}$. Heat of the Reaction $I_3^- = I_2 + I^-$. *J. Am. Chem. Soc.* **1951**, 73, 1842-1843, DOI 10.1021/ja01148a504.
- (3) Du, Y.; Wu, Y.; Liu, A.; He, L. Quaternary Ammonium Bromide Functionalized Polyethylene Glycol: A Highly Efficient and Recyclable Catalyst for Selective Synthesis of 5-Aryl-2-oxazolidinones from Carbon Dioxide and Aziridines Under Solvent-Free Conditions. *J. Org. Chem.* **2008**, 73, 4709-4712, DOI 10.1021/jo800269v.
- (4) Yang, Z.; He, L.; Peng, S.; Liu, A. Lewis basic ionic liquids-catalyzed synthesis of 5-aryl-2-oxazolidinones from aziridines and CO_2 under solvent-free conditions. *Green Chem.* **2010**, 12, 1850-1854, DOI 10.1039/C0GC00286K.
- (5) Wu, Y.; He, L.; Du, Y.; Wang, J.; Miao, C.; Lin, W. Zirconyl chloride: an efficient recyclable catalyst for synthesis of 5-aryl-2-oxazolidinones from aziridines and CO_2 under solvent-free conditions. *Tetrahedron*, **2009**, 65, 6204-6210, DOI 10.1016/j.tet.2009.05.034.
- (6) Varszegi, C. Olefin Aziridination with Ammonia and Amines. *PhD thesis*, KU Leuven (Belgium), **2009**.
- (7) Lebel, H.; Lectard, S.; Parmentier, M. Copper-Catalyzed Alkene Aziridination with N-Tosyloxycarbamates. *Org. Lett.* **2007**, 9, 4797-4800, DOI 10.1021/ol702152e.
- (8) Li, X.; Chen, N.; Xu, J. An Improved and Mild Wenker Synthesis of Aziridines. *Synthesis*, **2010**, 20, 3423-3428, DOI 10.1055/s-0030-1257913.
- (9) Nielander, A. C.; McEnaney, J. M.; Schwalbe, J. A.; Baker, J. G.; Blair, S. J.; Wang, L.; Pelton, J. G.; Andersen, S. Z.; Enemark-Rasmussen, K.; Čolić, V.; Yang, S.; Bent, S. F.; Cargnello, M.; Kibsgaard, J.; Vesborg, P. C. K.; Chorkendorff, I.; Jaramillo, T. F. A Versatile Method for Ammonia Detection in a

Range of Relevant Electrolytes via Direct Nuclear Magnetic Resonance Techniques. *ACS Catal.* **2019**, 9, 5797-5802, DOI 10.1021/acscatal.9b00358.

- (10) Sanders, J. K. M.; Hunter, B. K.; Jameson, C. J.; Romeo, G. Isotope effects on proton chemical shifts and coupling constants in the ammonium ions $^{15,14}\text{NH}_{4-n}\text{D}_n^+$. *Chem. Phys. Lett.* **1988**, 143, 471-476, DOI 10.1016/0009-2614(88)87398-6.